Improvements for the T0C+ Geometry of the Fast Interaction Trigger (FIT) Upgrade to ALICE at the CERN LHC

A Senior Project

By

Noah Miller

Advisor, Dr. Jennifer Klay

Department of Physics, California Polytechnic State University
San Luis Obispo

June 18, 2017

Approval Page

Title: Improvements for the T0C+ Geometry of the Fast Interaction Trigger (FIT) Upgrade to ALICE at the CERN LHC

Author: Noah Miller

Date Submitted: June 16, 2017

Senior Project Advisor: Dr. Jennifer Klay

_____

Signature

_____

Date

Contents

List of Tables

List of Figures

Acronym	Meaning
CERN	The European Organization for Nuclear Research (from the French abbreviation of **Conseil Européen pour la Recherche Nucléaire**)
LHC	The **Large Hadron Collider** at CERN
ALICE	**A Large Ion Collider Experiment** at the LHC at CERN
FIT	**Fast Interaction Trigger**, an upgrade to ALICE's trigger system
T0 / T0-Plus	Triggering detectors that measure the collision time of an event for ALICE's current triggering system and the FIT upgrade, respectively
V0 / V0-Plus	A forward detector system that features, among other things, multiplicity triggering, luminosity monitoring, and beam gas rejection for ALICE's current triggering system and the FIT upgrade, respectively
FMD	**Forward Multiplicity Detector**, a forward detector system currently in use at ALICE that features forward multiplicity determination
PMT	**Photomultiplier Tube**, a photon detector
MCP	**Microchannel Plate**, A component of the T0-Plus Cherenkov counter (MCP-PMT). May also be in reference to MCP-PMT, the Cherenkov counter module of the T0-Plus
TOF	The **Time of Flight** for a particle, a core measurement in particle physics experiments

Table 1: Acronyms

1 Introduction

1.1 The ALICE experiment at the CERN LHC

ALICE (A Large Ion Collision Experiment) is a general-purpose heavy-ion experiment at the LHC (Large Hadron Collider) at CERN (the European Center for Nuclear Research) that primarily investigates the strongly interacting matter and the quark-gluon plasma produced in nucleus-nucleus collisions.[1] Precise measurements are needed to understand the dynamics of the condensed phase of quantum chromodynamics. ALICE's design allows it to cope with the highest particle multiplicities anticipated for lead nuclei (Pb-Pb) collisions.[2] What differentiates ALICE from other experiments at the LHC is that it can identify lower energy particles than the other experiments, and as a consequence, ALICE usually runs at lower luminosities than other experiments at the LHC.

The LHC machine conducts maintenance and upgrades during long shutdown periods, and the experiments use those same windows to upgrade their detectors. Figure 1 shows the shutdown period schedule from 2010 to 2029 with the corresponding Pb-Pb integrated luminosity of the LHC for each run. The second major shutdown period of the LHC, which is planned to begin in July 2018 lasting until 2020, is referenced as "Long Shutdown 2" (LS2), and many upgrades to the LHC and its experiments are planned to be completed in this time. The LHC will progressively increase its luminosity with Pb beams, eventually reaching an interaction rate of about 50 kHz.[3] As seen in Figure 1, the ALICE Upgrade discussed in this paper is scheduled to take place during LS2.

1.2 The FIT Upgrade

The Fast Interaction Trigger (FIT) Upgrade is part of the planned upgrade of ALICE's three forward detector systems: the T0, the V0, and the FMD. These three detector systems can be seen in the cutout in Figure 2 and currently provide minimum bias trigger, multiplicity trigger, beam-gas event rejection, collision time for time of flight measurements, offline multiplicity, and event plane determination. The Fast Interaction Trigger Upgrade aims to replace these detectors with a single detector system that can provide these functionalities at the higher collision rates to be enabled by the LHC upgrade while also delivering on several other functionalities. This single detector system is called the Fast Interaction Trigger (FIT), and the FIT will be based on two sensor technologies that are more advanced than those

Figure 1: A timeline of the LHC's run periods and the corresponding integrated luminosities of each period.

used for the existing detectors, the V0 and T0. These two different parts of the FIT are referenced as the V0-Plus and the T0-Plus, and this paper will be focusing on proposed changes to T0-Plus. The FIT needs to fulfill additional requirements not possible with the current trigger detectors: determination of collision time for time of flight (TOF) measurements at a resolution better than 50 ps; insensitivity to after-pulses or other spurious signals; and must serve direct feedback to the LHC on luminosity and beam conditions. Along with software development for the FIT project, Cal Poly will begin work on T0A+ hardware development in 2018 under an NSF MRI grant to build the upgraded T0A-Plus detector. Dr. Jennifer Klay will lead this project to construct half of the T0A-Plus detector array. The FIT detector will be completed by 2019 to be installed into ALICE for operation by 2020.

1.3 The T0 and the T0-Plus

The T0 is currently a system of two arrays of detectors, T0A and T0C, that are at 370 cm and -70 cm[1] away from the interaction point (IP) respectively. Each array consists of 12 cylindrical Cherenkov counters equipped with a quartz radiator paired with a photomultiplier tube (PMT). The timing resolution of the T0 is better than 50 ps which improves at higher multiplicities along with its efficiency due to the T0 arrays' small acceptance. The T0's detector modules each have a 20-mm diameter window with 3-cm long segment of quartz.[4]

[1]The negative distance from the IP signifies the array being on the same side of the IP as the muon absorber (See Figure 2).

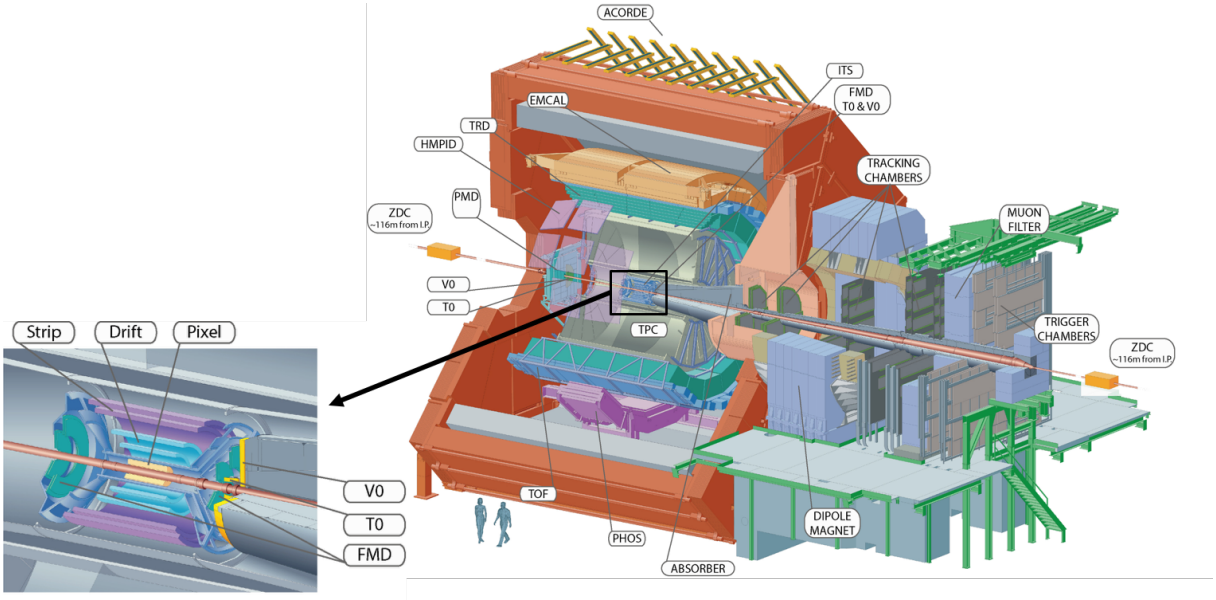

Figure 2: Diagram of the detectors of the current ALICE facility, before upgrades, with cutout of forward detector systems.

When a high-speed charged particle passes through a dielectric medium that has a high index of refraction, it can produce a cone of light if the particle is traveling faster than the speed of light for that medium. This light is called "Cherenkov Radiation". The closest physical analogy to this phenomenon outside of particle physics is the sonic boom, but instead of an object traveling faster than the speed of sound in the air producing sound waves, you have a particle producing light waves by traveling through a medium at speeds faster than light can travel in that medium. If quartz, for example, has an index of refraction of ≈ 1.43, a charged particle traveling at 0.7c or faster inside of it will produce a "light boom". The PMT coupled to the quartz radiator serves to amplify this light signal by converting it to an electrical current which is then recorded by the detectors electronics.

The T0-Plus will be a replacement of the T0 that is similar in composition but with improved technology; it will have two arrays of detectors, T0A+ and T0C+, that are at 328 cm and -80 cm from the IP, respectively. Each detector array layout (for the T0A+ and the T0C+) is shown in Figure 3, and the prototype of the detector module to be used for them can be seen in Figure 4. The T0+ is composed of fifty-four 60x60x64 mm^3 cubic quartz radiators coupled to microchannel plate photomultiplier tubes (MCP-PMT), with the T0A+ and T0C+ arrays having twenty-four and twenty-eight detectors respec-

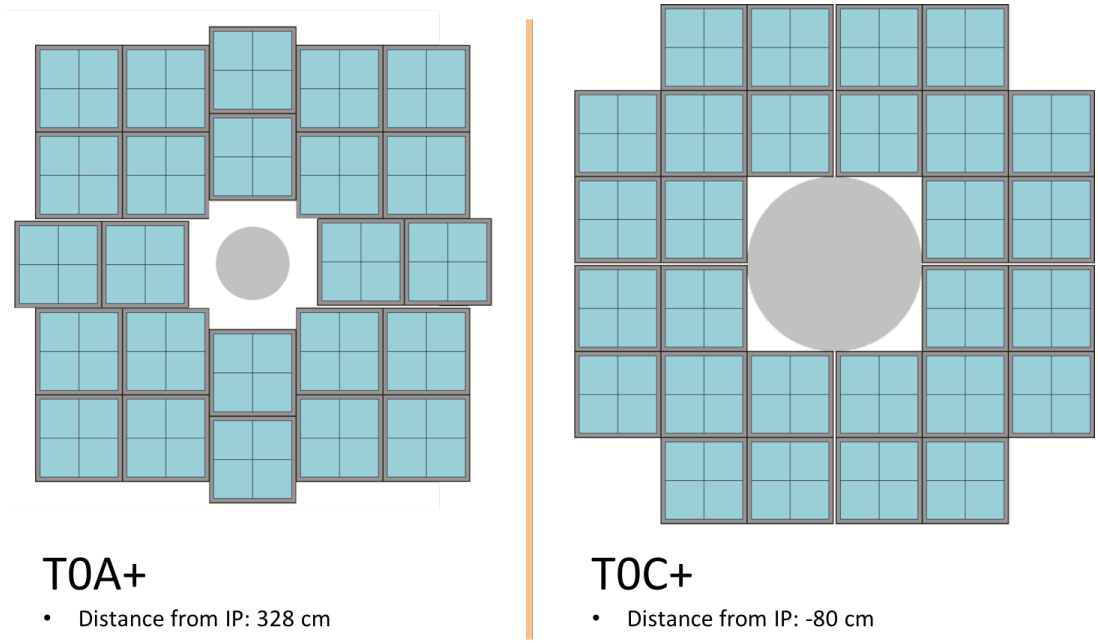

Figure 3: Proposed detector arrangement for each detector array of the T0-Plus, the T0A+ (left) and T0C+ (right), with their respective distances to the interaction point.

tively. Each detector module's face is divided into four quadrants, each 26.75 $\times$ 26.75 mm in area. The current quartz+PMT technology employed for the T0 is not capable of delivering on the goals of the FIT upgrade; for one, after-pulses are a serious issue with the current technology, especially at high multiplicities, where after-pulse amplitude becomes sizable enough to pass the discrimination level of the T0. Signals from the current T0 and V0 (as well as other PMT-based detectors in ALICE) systematically produce after-pulses with 20% of the main pulse amplitude some 20-120 ns after the main pulse arrival. It is a well known flaw with the technology and is attributed to the acceleration of ions triggering secondary signals. While after-pulses do not register at low multiplicities due to the discriminator, high multiplicity events have been shown to trigger multiple after-pulses for single signals which may overlap other main pulses.[1]

MCP-PMT-based technology is observed to have a significantly lower after-pulse rate at all studied multiplicities. The current candidate for the T0-Plus detector module is the XP85012 Planacon made by the Photonis Corporation, which has the largest relative (80 %) and absolute (53 mm $\times$ 53 mm) active area and the lowest price per surface of all the commercially available MCP-PMTs.

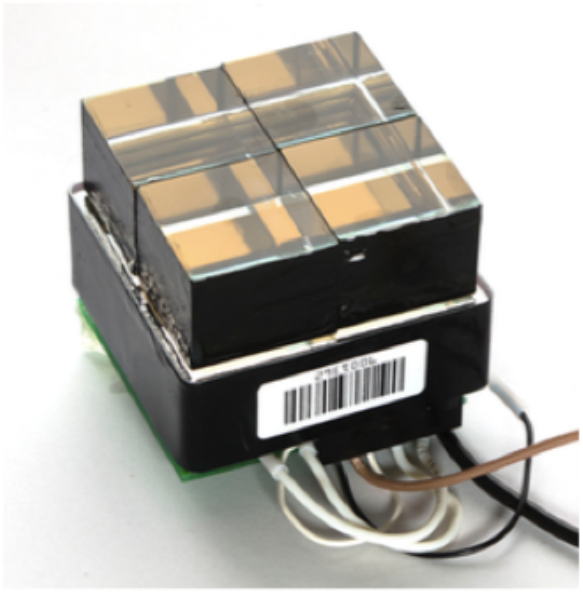

Figure 4: A T0-Plus detector module prototype: a Quartz Radiator coupled with a MCP-PMT.

1.4 Motivations for a New Geometry

While MCP-PMT-based technology is a clear improvement over the current technology in use, further investigation must be undertaken to evaluate its capabilities. One problem that has been investigated is how MCP signal strength is affected by the incident angle of the particle beam, even for central pixel events in the MCP window with no quartz radiator. As seen in Figure 5, the distribution of Cherenkov radiation produced by incoming particles changes as the incident angle of the beam becomes more oblique. More oblique angles reduce the signal strength of MCP's as seen in Figure 6. Figure 6 shows how each quadrant of an MCP's signal strength is decreased individually and collectively by higher incident angles. There are numerous hypotheses regarding why this phenomenon occurs. The reflectivity of the border between window and the photocathode of the PMT could be reducing the signal at oblique angles (and as such, the reflectivity is unclear), or it could be the result of variations in quantum efficiency for oblique photons. While the T0A+ array is too far from the interaction point for this phenomenon to substantially affect performance (the maximum incident angle at the far edge of the array is $\approx 2^{\circ}$), this phenomenon is especially troubling for the T0C+ as its proximity to the IP could lead to incident angles of up to 12.6°, potentially causing a full 20% reduction in signal strength.

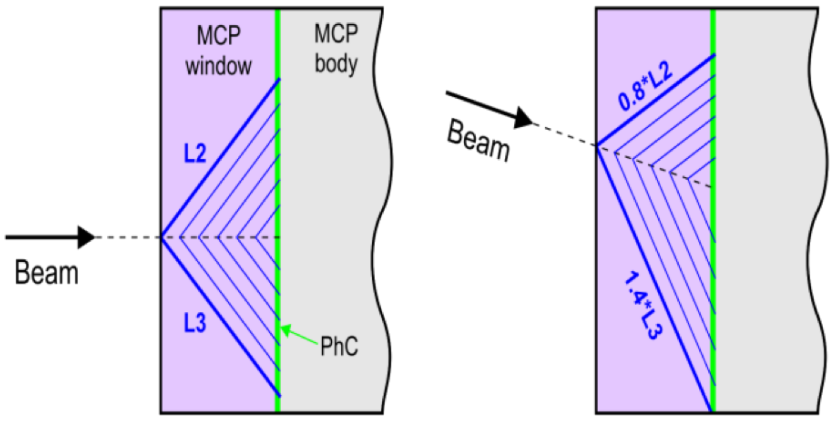

Figure 5: The distribution of light on the MCP in a Cherenkov event where the particle beam enters at different angles: normal (left) and oblique (right).

The proposed solution to this incident angle problem is a new, spherical detector array geometry for the T0C+. As seen in Figure 7 the current version of the T0C+ (referenced as Version 4) is a flat array, and the updated version (referenced as Version 5) is proposed to be spherically oriented towards the IP to reduce incident angles and regularize the distance between detectors and the IP. In this paper, we will discuss how this change was made and how it affected the function of the T0-Plus.

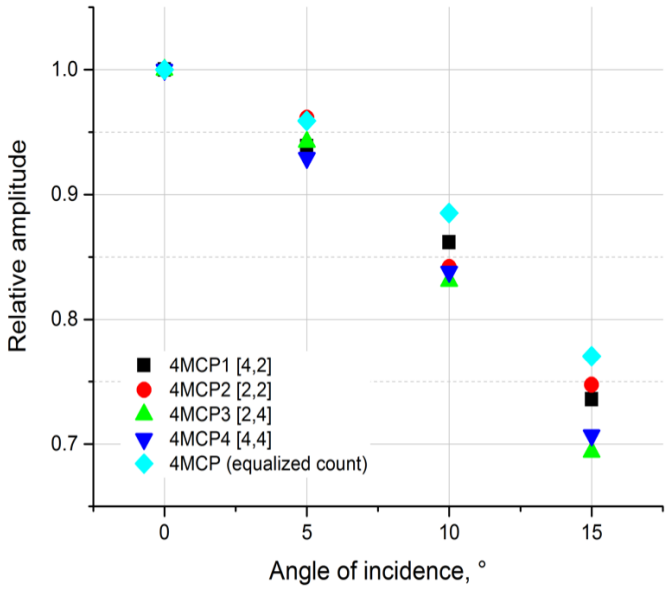

Figure 6: Simulation results showing the trend of amplitude vs. angle of incidence for MCP quadrants.

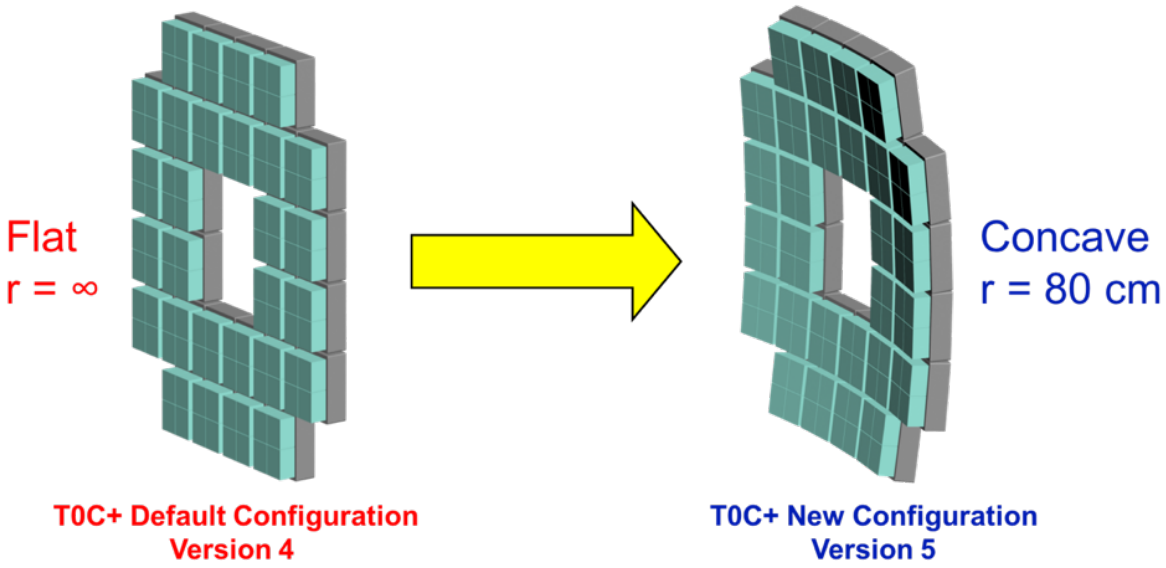

Figure 7: The Implemented change in geometry for the T0-plus C-Side detector array.

2 Methodology

2.1 AliRoot and AliFIT

All analysis and simulation in ALICE is run with the AliRoot software.[5] The AliRoot framework is based on Object-Oriented technology and dependent on the ROOT framework.[6]

> The ROOT framework provides a set of interacting classes and an environment for the development of software packages for event generation, detector simulation, event reconstruction, data acquisition, and a complete data analysis framework. ROOT is written in C++ and offers an efficient hierarchical object store with a complete set of object containers, a C++ interpreter allowing one to use C++ as scripting language, advanced statistical analysis tools (multidimensional histograms, several commonly used mathematical functions, random number generators, multi-parametric fit, minimization procedures, cluster finding algorithms etc.), hyperized documentation tools, geometrical modeling, and advanced visualization tools.[5]

Each detector in ALICE has its own set of objects and macros in AliRoot to run simulations or

analyses on reconstructed data, and users can themselves create macros to do their own analyses and simulations. For the FIT, detector simulations (and, eventually, data reconstructions) are run with AliRoot macros that load AliFIT files. These files contain all the information about the detectors that make up the FIT: their positions in ALICE, their materials, their optical properties, etc. To change the geometry of the T0C+ detector array, the AliFIT file must be changed to log in the updated positions and orientations of each detector in the array. In the AliRoot software, detector position and orientation are determined by two objects: TGeoTranslations and TGeoRotations, respectively. In this section, we will show how the proposed change in the T0C+ geometry was mapped to translations and rotations for implementation into the AliFIT file.

2.2 Translations

Detector positions are entered into the TGeoTranslation object as simple xyz-coordinates. The z-axis runs along the mean of the center beam pipe of ALICE, and the origin is set at the nominal interaction point (the designed IP). The y-axis protrudes vertically from the IP as the x-axis protrudes horizontally. For our purposes, all values of z for individual detectors are treated as positive as the T0C+ array is treated as a mother volume and has its own z-coordinate in the AliFIT file. Each detector in the array has a node position that is in the center of the detector's volume to tell AliRoot where to place that detector in the mother volume of the T0C+ detector array.

To determine the node position of each detector in the array, the angle between two adjacent detectors on a 80-cm sphere is first calculated. Figure 8 shows the geometry of two adjacent detectors where R is the radius of the sphere, s is the width of each detector, and ϕ is the angle between a detector's tangent point and the contact point of both detectors. The angle between adjacent detectors then is $\theta = 2\phi$, or

$$\theta = 2 \arccos\left(\frac{R}{\sqrt{\left(\frac{s}{2}\right)^2 + R^2}}\right) \tag{1}$$

Using $s = 5.9$ cm and $R = 80$ cm, the angle between two adjacent detectors is $\theta = 4.22°$.

This angle can be used to determine the xyz-coordinates for each detector in the array by assigning each detector a position in a 2D-grid with indices, (n, m), that range from -3 to 3. Figure 9 shows how each detector node was assigned its index for determining the xyz-coordinates. Each node's xy-

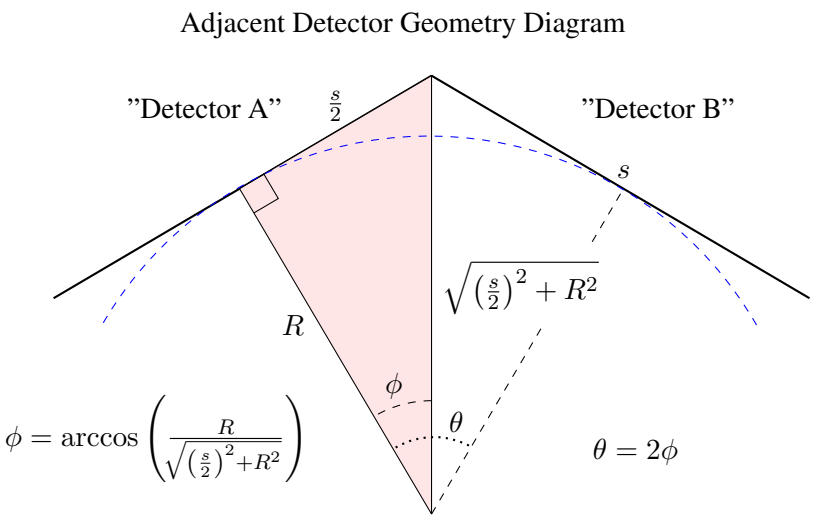

Figure 8: A diagram showing how the angle between two adjacent detectors is calculated (not to scale).

coordinates are functions of its grid position, and its z-coordinates are a function of its xy-coordinates, or

$$x_n = R \cdot \sin\left(\left[1 - \frac{1}{2|n|}\right] \cdot n\theta\right), \quad y_m = R \cdot \sin\left(\left[1 - \frac{1}{2|m|}\right] \cdot m\theta\right) \tag{2}$$

$$z_{nm} = \sqrt{R^2 - x_n^2 - y_m^2} \tag{3}$$

where $R = 80$ cm and $\theta = 4.22°$. With the node position of each detector determined, the orientation for each face can also be calculated.

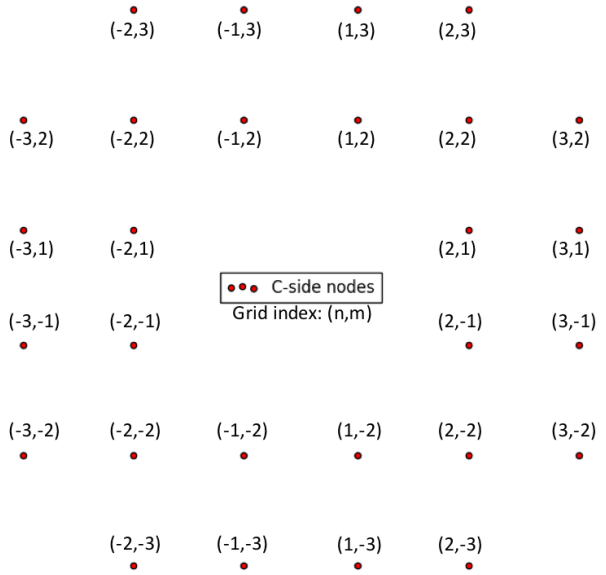

Figure 9: Indexing of detector node positions.

2.3 Rotations

The TGeoRotation object in AliRoot can take either Euler angles or GEANT-3 angles[3], but for our purposes, Euler angles are preferred. Euler angles determine orientation with three angles, α, β, and γ, where each rotation is applied in sequence. As seen in Figure 10, the first rotation shifts the x-axis along the xy-plane by α to a new x-axis, N. The second rotation shifts the z-axis by β by rotating about N to a new z-axis, Z. The third and final rotation shifts the x-axis (currently N) by γ about Z to a new x-axis, X. These angles are functions of node position expressed by the following equations:

$$\alpha_{nm} = \arctan\left(\frac{y_m}{x_n}\right) - \frac{\pi}{2} \tag{4}$$

$$\beta_{nm} = \arccos\left(\frac{z_{nm}}{R}\right) \tag{5}$$

$$\gamma_{nm} = -\alpha_{nm} \tag{6}$$

[3]GEANT-3 is the simulation package that stands for **"GEometry ANd Tracking"** and is used by AliROOT for generated particle transportation [5]. This package is discussed more in Section 3.1.

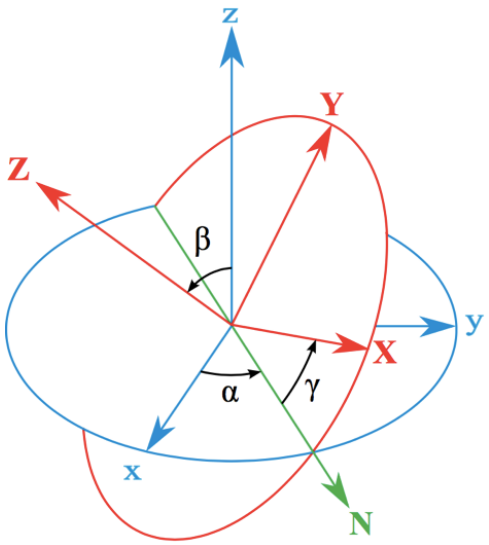

Figure 10: Euler angles diagram.[2]

where $R = 80$ cm and x_n, y_n, and z_{nm} are determined by Equations 2 and 3. Equation 4 derives from the equation for the angle ϕ that sits between the y-axis and x-axis in spherical coordinates with $\phi = \arctan\left(\frac{y}{x}\right)$ and $\alpha = \phi - \frac{\pi}{2}$ because α protrudes from the x-axis rather than the y-axis. Equation 5 derives from the equation for θ in spherical coordinates, $\theta = \arccos\left(\frac{z}{R}\right)$. Equation 6 is simply the negative of α to finish orienting the detector by correcting the intial rotation of α.

2.4 Translations Revisited

With each of the Euler angles for the orientation determined, a correction to the translations must be made. As a property of the node positions being in the exact center of the individual detector volumes, the current translations have each detector overlapping adjacent detectors at their faces since the method for determining their positions did not account for the 2.5 cm distance between the face of the detector and its node position within its volume. However, with the Euler angles, this is easy to correct for. Simply adding 2.5 cm to the radius and calculating x_{nm}, y_{nm}, and z_{nm} as functions of α_{nm} and β_{nm} can determine translations with no overlap, or

$$x_{nm} = R_c \cos\left(\alpha_{nm} + \frac{\pi}{2}\right) \cdot \sin(-\beta_{nm}), \quad y_{nm} = R_c \sin\left(\alpha_{nm} + \frac{\pi}{2}\right) \cdot \sin(-\beta_{nm}) \tag{7}$$

[3]Image Credit for Figure 10 to Lionel Brits; 9 January 2008[7]

$$z_{nm} = R_c \cos(\beta_{nm}) \tag{8}$$

where R_c is $R + 2.5$ cm = 82.5 cm, and α_{nm} and β_{nm} are determined by Equations 4 and 5 respectively. The translation and rotation data for the Version 5 T0C+ geometry was inputed into the AliFIT file as:

```
//Alpha, Beta, and Gamma angles for the C side Rotations (all angles in degrees)
Double_t ac[28] = { 211.0555505 , 191.37002946, 348.62997054, 328.9444495,
            238.9444495 , 225.  , 198.46612083, 341.53387917,
            315.     , 301.0555505 , 258.62997054, 251.53387917,
            288.46612083, 281.37002946, 281.37002946, 288.46612083,
            251.53387917, 258.62997054, 301.0555505 , 315. ,
            341.53387917, 198.46612083, 225. , 238.9444495 ,
            328.9444495 , 348.62997054, 191.37002946, 211.0555505 };
Double_t bc[28] = {12.35160924, 10.77300323, -10.77300323, -12.35160924,
            12.35160924, 8.978165 , 6.68091565, -6.68091565,
            -8.978165 , -12.35160924, 10.77300323, 6.68091565,
            -6.68091565, -10.77300323, 10.77300323, 6.68091565,
            -6.68091565, -10.77300323, 12.35160924, 8.978165 ,
             6.68091565, -6.68091565, -8.978165 , -12.35160924,
            12.35160924, 10.77300323, -10.77300323, -12.35160924};
Double_t gc[28] = {-211.0555505,-191.37002946,-348.62997054,-328.9444495,
            -238.9444495 , -225. , -198.46612083, -341.53387917,
            -315.     , -301.0555505 , -258.62997054, -251.53387917,
            -288.46612083, -281.37002946, -281.37002946, -288.46612083,
            -251.53387917, -258.62997054, -301.0555505 , -315. ,
            -341.53387917, -198.46612083, -225. , -238.9444495 ,
            -328.9444495 , -348.62997054, -191.37002946, -211.0555505 };
//x, y, and z positions for the C side Translations (all coordinates in cm)
Double_t xc2[28] = { -9.10385087, -3.04012128, 3.04012128, 9.10385087,
             -15.11813129, -9.10385087, -3.04012128, 3.04012128,
              9.10385087, 15.11813129, -15.11813129, -9.10385087,
              9.10385087, 15.11813129, -15.11813129, -9.10385087,
              9.10385087, 15.11813129, -15.11813129, -9.10385087,
             -3.04012128, 3.04012128, 9.10385087, 15.11813129,
             -9.10385087, -3.04012128, 3.04012128, 9.10385087};
Double_t yc2[28] = { 15.11813129, 15.11813129, 15.11813129, 15.11813129,
              9.10385087, 9.10385087, 9.10385087, 9.10385087,
              9.10385087, 9.10385087, 3.04012128, 3.04012128,
              3.04012128, 3.04012128, -3.04012128, -3.04012128,
             -3.04012128, -3.04012128, -9.10385087, -9.10385087,
             -9.10385087, -9.10385087, -9.10385087, -9.10385087,
             -15.11813129, -15.11813129, -15.11813129, -15.11813129};
Double_t zc2[28] = { 80.59039648, 81.04597318, 81.04597318, 80.59039648,
              80.59039648, 81.4892005 , 81.93978009, 81.93978009,
              81.4892005 , 80.59039648, 81.04597318, 81.93978009,
              81.93978009, 81.04597318, 81.04597318, 81.93978009,
              81.93978009, 81.04597318, 80.59039648, 81.4892005 ,
              81.93978009, 81.93978009, 81.4892005 , 80.59039648,
              80.59039648, 81.04597318, 81.04597318, 80.59039648};

 //Size of TGeoTranslation set to 52 to include 24 A-Side detectors and 28 C-Side Detectors
TGeoTranslation *tr[52];
TString nameTr;

 //TGeoRotation object's size set to 28 as C-Side is the only array with rotated detectors
TGeoRotation *rot[28];
TString nameRot;

//TGeoCombiTrans allows translation and rotation data to be stored in one object that sets detector relative position and
     rotation inside C-Side mother volume
TGeoCombiTrans *com[28];

 //C Side Transformations (Index starts at 24)
for (Int_t itr=24;itr<52; itr++) {
  //Set names for each translation and rotation
  nameTr = Form("0TR%i",itr+1);
  nameRot = Form("0Rot%i",itr+1);

  //Store rotation data into TGeoRotation Object and register it
  rot[itr-24] = new TGeoRotation(nameRot.Data(),ac[itr-24],bc[itr-24],gc[itr-24]);
  rot[itr-24]->RegisterYourself();

  //Store translation data into TGeoTranslation Object and register it
  tr[itr] = new TGeoTranslation(nameTr.Data(),xc2[itr-24],yc2[itr-24], (zc2[itr-24]-80.) );
```

```
    tr[itr]->RegisterYourself();

    //Store translation and rotation data in TGeoCombiTrans object with z-coordinates adjusted to be zero at the center of
         the C-Side mother volume
    com[itr-24] = new TGeoCombiTrans(xc2[itr-24],yc2[itr-24], (zc2[itr-24]-80),rot[itr-24]);

      //Registering TGeoCombiTrans nodes in stlinC
    TGeoHMatrix hm = *com[itr-24];
    TGeoHMatrix *ph = new TGeoHMatrix(hm);
    stlinC->AddNode(ins,itr,ph);
  }
```

With the position and orientation data for each detector input into the AliFIT file, simulations with the new geometry can be conducted to compare the Version 5 geometry with the flat Version 4 geometry that preceded it.

3 Simulations

3.1 AliRoot and Simulation Macros

With a working AliRoot environment, running simulations is done with macros that use the AliSimulation object. AliRoot simulations follow this process (also summarized in the flowchart of Figure 11:

1. **Event generation**: creates a list of particles to simulate. This particle list could come from a particle gun or a Monte Carlo generator like PYTHIA. Particle type, start point (x, y, z), and momentum vector (p_x, p_y, p_z) are selected. This step outputs a Kinematics.root file.

2. **Particle transport**: tracks energy loss and deposition by the particles traveling through detector geometry via the GEANT-3 software package. GEANT-3 is a particle transport model that attempts to simulate the interaction of particles with matter, keeping track of the locations of the hits within detection volumes and the amount of energy deposited. This step outputs a DETECTOR.Hits.root file.

3. **Detector simulation**: simulates how well the detector can reconstruct the deposited energy, including the digitization process, electronics noise addition, time delays, etc. This step outputs a DETECTOR.Raw.root file which is in the same format as the raw output from the detector would be in a real experiment, and this file is fed into the reconstruction process.

4. **Reconstruction**: takes either the output of the digitization step or raw data from the real experiment and reconstructs the particle trajectories. This step outputs an AliESDs.root file which is

formatted for analysis.

5. **Evaluation**: connects the generated particle information in the Kinematics.root file (the output of step 1) with either the DETECTOR.Hits.root file (the output of step 2) or the AliESDs.root file (the output of step 4) to determine how well a given detector measures it.

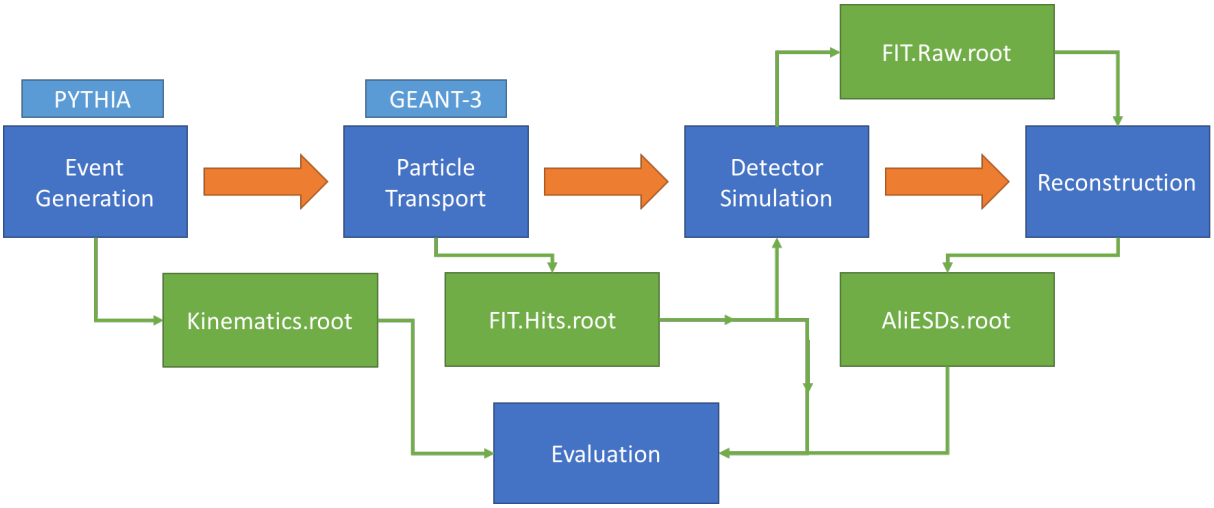

Figure 11: A flowchart showing how simulations are run to evaluate detectors

Simulation runs with generated data output four .root files: a Kinematics.root file that contains all of the information about the particles in the simulation, a DETECTOR.Hits.root file that contains all the information about all the simulated hits for the given detectors that came from the generated particles, a DETECTOR.Raw.root file that contains the output of the detector simulation and matches the real raw data format, and an AliESDs.root file that is used for analysis. For the FIT, our current simulation macros output a Kinematics.root file and a FIT.Hits.root file which are used to analyze how changes to the AliFIT file affect the FIT's performance. Colleagues in the FIT development project for ALICE ran the simulations referenced in this paper to compare the Version 4 and Version 5 FIT geometries.

3.2 Efficiency Comparison between Version 4 and Version 5

A simulation of $19,000$ proton-proton events at 13 TeV was done with both the Version 4 AliFIT file and the Version 5 AliFIT to analyze potential effects the change in C-Side geometry may have had on the FIT's efficiency. There are two measures of efficiency for the T0+ as it's composed of two detector

arrays on opposite sides of the interaction point: AND (&) signal efficiency and OR (||) signal efficiency. The & signal reliably tells ALICE that a collision event that generates many particles did occur, but with lower efficiency, and the || signal tells ALICE that an event that generates many particles occurred, but has more background from beam-gas interactions or pile-up events not associated with the collision of interest. Figure 12 shows the efficiency of the FIT for events with different numbers of primaries[4] (i.e. particles produced in the event) where the & signal efficiency is shown on the left and the || signal efficiency is shown on the right. The results of the simulation for both the Version 4 geometry and the Version 5 Geometry are shown in red and blue respectively. Table 2 shows the average efficiencies of each geometry version for each signal type. Both the plots and the table show that the change in geometry had no detrimental effect on the efficiency of the FIT.

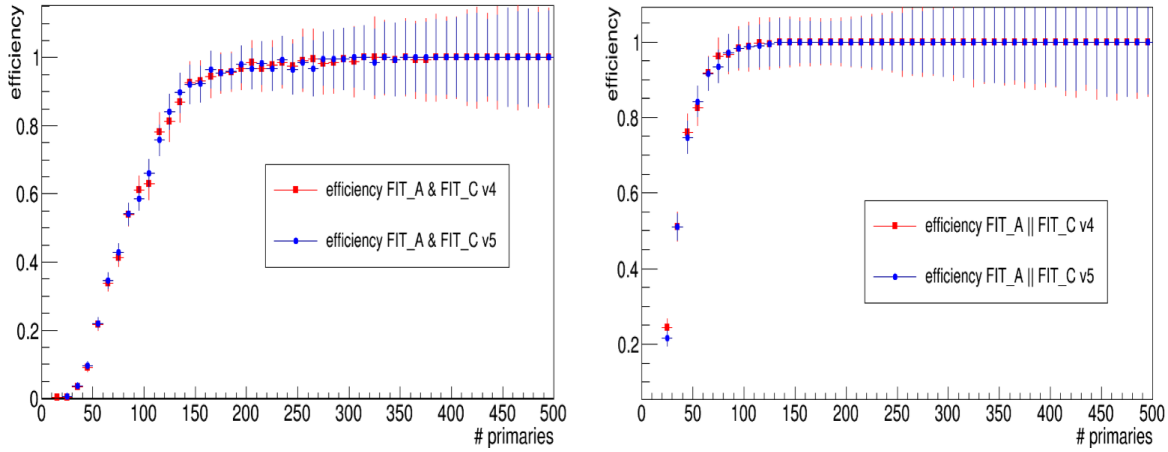

Figure 12: Efficiency comparison for version 4 geometry and version 5 geometry for conjoined A-side and C-side signal (left) and either-or A-side and C-side signal (right)

Signal Type	v4 Efficiency Average	v5 Efficiency Average
&	75.4 %	75.2 %
||	91.6 %	91.7 %

Table 2: Efficiency averages for geometry version comparison.

[4]Primaries are specifically particles that were initially produced by the collision at the interaction point. This is different from many of the particles in experiments that are "secondary", that are produced by the primaries decaying, converting, or interacting with detector materials.

3.3 Time of Flight Comparison between Version 4 and Version 5

A similar simulation was run to analyze how time-of-flight (TOF) measurements could be affected by the change in the geometry. Figure 13 shows the results of the simulation where the TOF averages for each MCP quadrant in the T0C+ are shown for the Version 4 geometry (shown in red) and the Version 5 geometry (shown in blue). From the figure, the TOF distribution of the v4 geometry has clear peaks for quadrants near the outer corners of the T0C+ whereas the TOF distribution for the v5 geometry has less pronounced peaks for those quadrants. This result can be explained by Figure 14, which is a histogram showing the total distances that each particle in the simulation traveled before they were detected by the T0C+ for the Version 4 geometry (shown in red) and the Version 5 geometry (shown in blue). As expected of a spherical geometry, the distance traveled by each particle before it hits a detector is far more regular than a flat geometry which has detectors farther away from the IP at the outer corners of the array. This increased regularity of the TOF distribution is a clear improvement on the old geometry's performance.

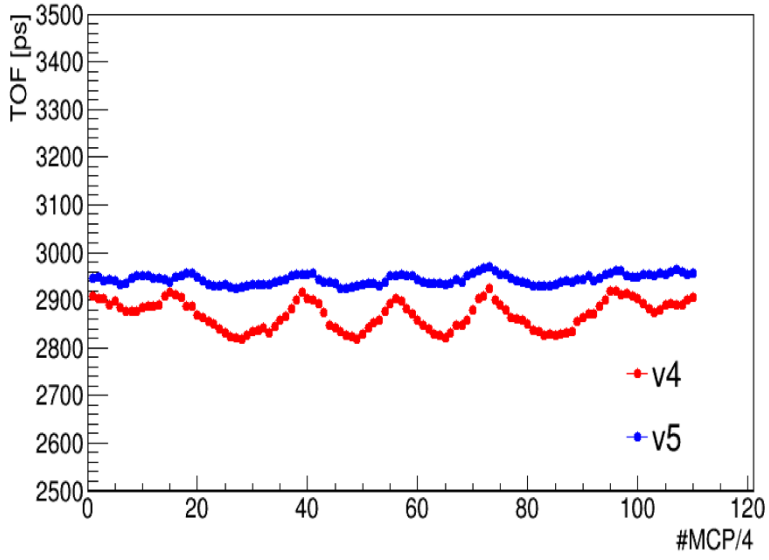

Figure 13: Plot showing time of flight results from a simulation of both Version 4 and Version 5 geometries.

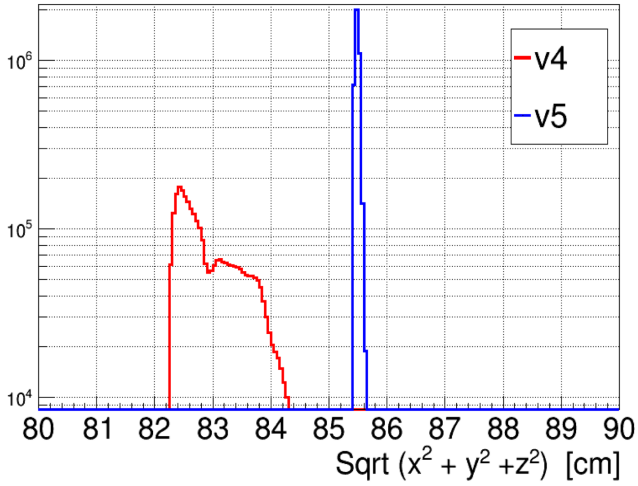

Figure 14: Plot showing travel distance results from a simulation of both Version 4 and Version 5 geometries.

4 Discussion

The results of these early simulations are promising for the new geometry as there are no tangible losses in efficiency for the change and the distribution of time of flight measurements for the T0C+ has markedly improved. A more regular TOF distribution for the T0C+ will allow for easier comparisons between particle hits which enables triggering on more interesting events than ALICE has been able to access before. The efficiency plots show that there is no degradation with the new geometry. Coupled with the fact that the MCP-PMTs in the T0+ dont run the risk of creating significant after-pulses like the original T0 means that the new detector will operate more effectively in the higher luminosity environment. Both of these early results show much promise for the new geometry and the T0C+.

5 Conclusions

The LHC Upgrade during LS2 will enable higher luminosity studies in particle physics for all LHC experiments, and ALICE's upgrades aim to take full advantage of it. Without effective triggering, however, ALICE's other upgrades will be useless, making the Fast Interaction Trigger critical to ALICE's program. Early simulations suggest that the Version 5 geometry is a clear improvement over the original flat

Version 4 geometry in that it provides more stable TOF measurements, and with it, the FIT development project has gotten closer to achieving the desired timing resolution for the FIT. As FIT development ramps up, however, the optical properties of the quartz radiators and the optical connection to the MCP are going to be further updated and refined before more simulations are run to determine detector performance. Realistic optical data for the MCP-PMT is being inputed into the AliFIT file now, and once the results of those simulations are compared to the results of beam tests with the MCP-PMTs, we'll have a good idea of how well the FIT will perform. As the software is being refined to satisfaction, the hardware development for the FIT will also move forward.

When the FIT is installed and ALICE is fully upgraded at the end of LS2, ALICE can start studying even higher energy density collisions to explore the exciting properties of quark-gluon plasma and search for answers to some of the most interesting questions about the beginning of our universe.

References

[1] ALICE collaboration et al. Upgrade of the alice readout & trigger system. *Technical design report, CERN-LHCC-2013-019, ALICE-TDR-015*, 2013.

[2] B Alessandro, F Antinori, JA Belikov, C Blume, A Dainese, P Foka, P Giubellino, B Hippolyte, C Kuhn, G Martínez, et al. Alice: Physics performance report, volume ii. *Journal of Physics G: Nuclear and Particle Physics*, 32(10):1295, 2006.

[3] ALICE collaboration et al. Letter of intent for the upgrade of the alice experiment. *Tech. Rep., CERN-LHCC-2012-012, LHCC-I-022*, 2012.

[4] ALICE collaboration et al. Alice forward detectors: Fmd, to and vo: Technical design report. Technical report, CERN-LHCC-2004-025, http://cdsweb. cern. ch/record/781854, 2004.

[5] ALICE Collaboration et al. Technical design report for the alice computing, cern/lhcc 2005-18; aliroot, alice offline simulation, reconstruction and analysis framework. *aliceinfo. cern. ch/Offline/S*.

[6] Rene Brun and Fons Rademakers. Rootan object oriented data analysis framework. *Nuclear Instruments and Methods in Physics Research Section A: Accelerators, Spectrometers, Detectors and Associated Equipment*, 389(1-2):81–86, 1997.

[7] Wikipedia. Euler angles — wikipedia, the free encyclopedia, 2017. [Online; accessed 6-June-2017].